Dynamic study on the transformation process of gold nanoclusters

2014 Nanotechnology 25 445705

(http://iopscience.iop.org/0957-4484/25/44/445705)

IOP Publishing Nanotechnology
Nanotechnology **25** (2014) 445705 (6pp) doi:10.1088/0957-4484/25/44/445705

Dynamic study on the transformation process of gold nanoclusters

Xiaoqian Ma[1], Xiaoming Wen[2,4], Yon-Rui Toh[1], Kuo-Yen Huang[1], Jau Tang[1,3] and Pyng Yu[1,4]

[1] Research Centre for Applied Science, Academia Sinica, Taipei, Taiwan
[2] Australian Centre for Advanced Photovoltaics, University of New South Wales, Sydney 2052, Australia
[3] Institute of Photonics, National Chiao-Tung University, Hsinchu, Taiwan

E-mail: xwen@unsw.edu.au and d91223002@ntu.edu.tw

Received 15 May 2014, revised 16 August 2014
Accepted for publication 10 September 2014
Published 16 October 2014

Abstract

In this paper, the transformation process from Au_8 to Au_{25} nanoclusters (NCs) is investigated with steady state fluorescence spectroscopy and time-resolved fluorescence spectroscopy at various reaction temperatures and solvent diffusivities. Results demonstrate that Au_8 NCs, protected by bovine serum albumin, transform into Au_{25} NCs under controlled pH values through an endothermic reaction with the activation energy of 74 kJ mol^{-1}. Meanwhile, the characteristic s-shaped curves describing the formation of Au_{25} NCs suggest this process involves a diffusion controlled growth mechanism.

Keywords: gold nanocluster, time-dependent fluorescence spectra, structure transformation, growth mechanism

(Some figures may appear in colour only in the online journal)

1. Introduction

Gold nanoclusters (NCs) have drawn significant research interest due to their characteristic optical and physical properties, and their many potential applications including imaging, catalysts, sensing and photonics [1–5]. These NCs containing only a few, or tens, of atoms are distinctly different from bulk metals or larger nanoparticles. They possess discrete energy levels and molecule-like properties in the absorption and fluorescence feature [6–9]. A series of atomically precise gold NCs protected by ligands have been obtained with well-defined molecular compositions as well as distinct luminescence characteristics [10]. Bovine serum albumin (BSA), a well known blood protein, is a widely used ligand with various advantages, such as low cost, stability and numerous biochemical applications [11]. BSA-protected gold NCs are highly luminescent and stable from acidic environment to alkali environment, providing promising applications in bioimaging and photonics[12–14]. A simple synthetic method of preparing Au_{25} NCs has been reported by adding Au(III) to BSA solution with a finally adjusted pH value of around 12 [14]. Furthermore, researchers have demonstrated that the structure and properties of gold NCs can be greatly affected by the pH of the environment during synthesis process [15–18]. Gold NCs with blue, green and red emissions can be obtained at different pHs [15]. Small gold NCs prepared at pH 8 grow into bigger ones using a one-step technique; increasing the pH value of the original solution [16, 17]. Different sized gold NCs are prepared by tailoring the protein conformation [19]. Many efforts have been made to understand the growth mechanism of gold NCs, because it is of critical importance for both the synthesis and potential applications of gold NCs. However, results focusing on the mechanism of the formation and transformation processes of gold NCs are still very limited and challenging, mainly due to the complexity of the synthesis processes and the lack of the dynamic information.

In this work, we investigate the dynamic process of transformation from Au_8 NCs to Au_{25} NCs using the time-dependent fluorescence technique. The observed experimental results provide a detailed insight into the dynamic formation

[4] Author to whom any correspondence should be addressed.

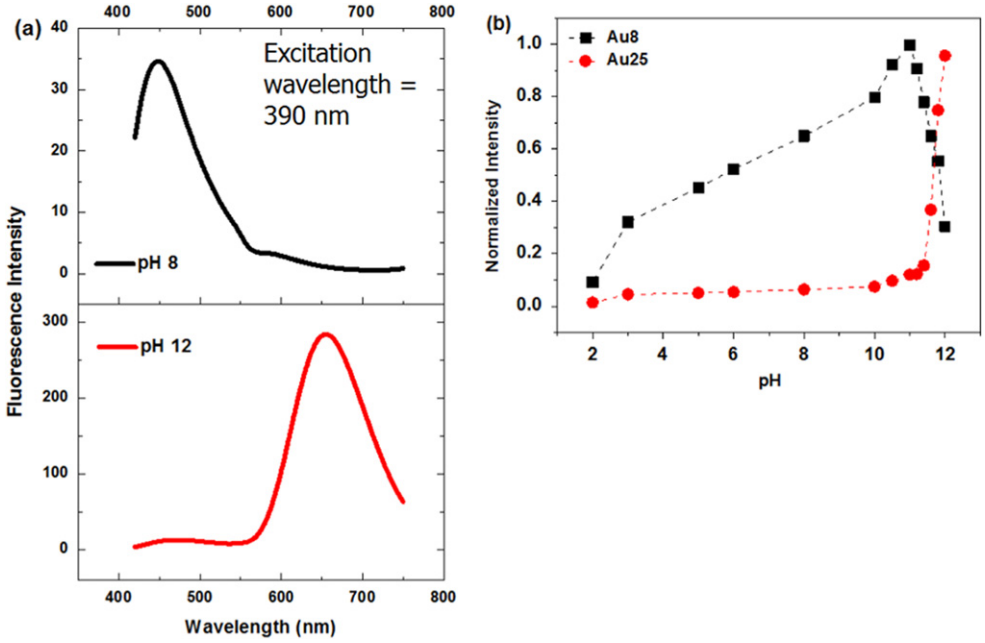

Figure 1. (a) Fluorescence emission spectra of gold NCs at pH = 8 and 12; (b) normalized peak intensities for Au_8 NCs and Au_{25} NCs as a function of the pH value.

of gold NCs. Here we proposed a mechanism for atomically precise gold NCs transformation to elucidate this process.

2. Materials and methods

BSA protected gold NCs are synthesized as described by Guével *et al* in 2011 [17]. Typically, 5 mL of 10 mM $HAuCl_4$ was mixed with 5 mL of 50 mg mL^{-1} BSA. 50 microliters of ascorbic acid was added dropwise and the solution was kept at 37 °C overnight in an incubator. A series of Au-BSA solutions were prepared with different pHs ranging from 2 to 12 by adding HCl or NaOH as required.

The fluorescence spectra were collected using a JASCO FP-6300 spectrophotometer with the solution in a 10 cm cuvette excited by a 390 nm laser. The lifetimes were measured by the time-correlated single photon counting (TCSPC) technique on a Microtime-200 system (Picoquant). The fluorescence quantum yield of Au NCs solution was determined as Au_8: 9.8% and Au_{25}: 3.9% by comparing the standard dye of Rhodamine 6G using the same fluorescence spectrometer.

3. Results and discussion

3.1. Gold NCs' transformation under controlled pH

The steady state fluorescence emission spectra of the solution are recorded as a function of pH to investigate the effects of pH on the structure and properties of gold NCs. Researchers have clarified the number of gold atoms in the NCs, as well as their featured luminescence properties, with x-ray photon electron spectroscopy (XPS), matrix-assisted laser desorption ionization time of flight mass spectroscopy (MALDI-TOF MS) and fluorescence spectroscopy [14, 17, 20–24]. When the pH is 8, only one primary emission peak attributed to Au_8 NCs is shown around 450 nm (black trace, figure 1(a)). As the pH increases to 12, an additional peak appears around 650 nm, which has been attributed to Au_{25} NCs (red trace, figure 1(a)). Figure 1(b) summarizes the relationship between the peak intensities of gold NCs and pH. It reveals that the peak intensities from Au_8 NCs initially rise steadily and then immediately drop down once the pH reaches 11. Meanwhile, the peak intensities from Au_{25} NCs are initially almost zero but dramatically increase. Those results indicate that the transformation process involves the consumption of Au_8 NCs and the formation of Au_{25} NCs as the pH is over 11. When adding $HAuCl_4$ to the aqueous BSA solution, Au_8 NCs are formed in the solution. It has been confirmed that Au_8-BSA NCs consist of only Au(0) [17, 25]. The disulfide bonds of BSA are expected to be hidden within the secondary structure [26]. Therefore, the Au-S covalent bond cannot be formed in acidic environment. Only a weak non-covalent interaction exists between Au(0) and the protein. The conformation change of BSA, after the gold NCs are labelled in alkali environment, was reported demonstrating the high degree of oxidation of sulfur for gold NCs [17, 19, 27]. Thus, Au-S covalent bonds are generated from the strong interaction between small gold NCs and the sulphur groups in the cysteine of BSA to form the larger gold NCs at the pH of 12, resulting in the rapid decreasing of florescence intensity at 450 nm and the significant increasing of fluorescence intensity at 650 nm. Here, the gold NCs' solution at pH = 8 is considered as the Au_8 NCs' solutions used for the following investigation, while that at pH = 12 is treated as the Au_{25} NCs' solutions although a smallnumber of Au_8 NCs may still coexist.

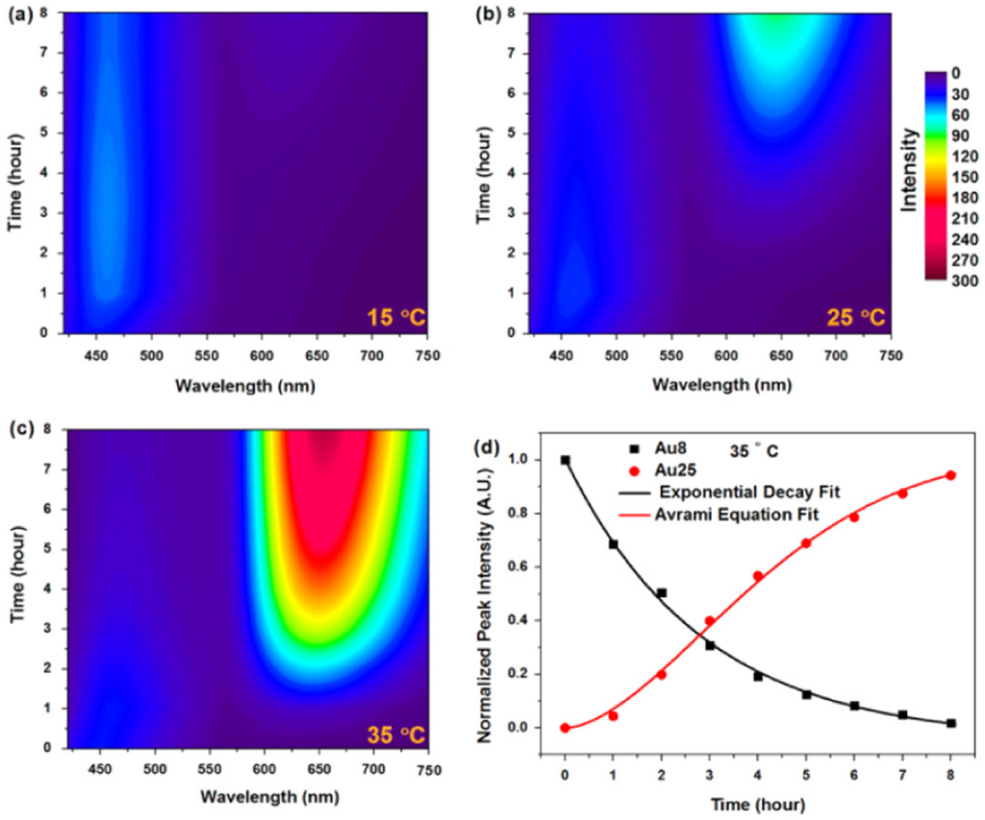

Figure 2. 2D fluorescence spectra contour plots in relation to the wavelength and time of the gold NCs' transformation process for 8 h at (a) 15 °C, (b) 25 °C and (c) 35 °C with excitation at 390 nm. (d) Normalized peak intensities and the corresponding fitting curves for Au_8 NCs and Au_{25} NCs as a function of time at 35 °C.

3.2. Effects of reaction temperature

NaOH is added into the Au_8 NCs' solution at pH = 8 to obtain a new pH value of 12. Then, three samples are prepared from the mixture and kept for 8 h at 15 °C, 25 °C and 35 °C, respectively. The kinetic photoluminescence spectra were recorded as a function of time as shown in figure 2. The fluorescence spectra contour plots of gold NCs with excitation at 390 nm (figures 2(a)–(c))indicate that higher temperature accelerates the decline of the emission band from Au_8 NCs. Correspondingly, the emission band from Au_{25} NCs appears earlier and grows faster at a higher temperature, demonstrating that the transformation process is an endothermic reaction. As shown in figure 2(c) at the emission spectral evolution at 25 °C, the intensity of Au_8 at 460 nm gradually decreases while that of Au_{25} at 650 nm gradually increases. The spectral shape and wavelength of the peaks do not evidently change. The normalized peak intensities (I) for Au_8 NCs and Au_{25} NCs as a function of time (t) can be obtained using the emission spectra (figure 2(d)). The decay of Au_8 NCs' intensity is well fitted with exponential decay function,

$$I = e^{-kt} \tag{1}$$

and the growth of Au_{25} NCs' intensity is well fitted with the Avrami equation

$$I = 1 - \exp\left[-(Kt)^n\right] \tag{2}$$

where k is the rate constant, K the apparent rate constant and n Avrami component. Thus, Au_8 NCs' consumption can be considered as a first-order reaction with the reaction rate only depending on a single reactant, Au_8 NCs. Meanwhile, the characteristic S-shaped curve of Au_{25} NCs' formation indicates three stages may exist sequentially. At the very beginning, a limited number of nuclei coming from Au8 NCs are generated, which leads to the initially slow rate. Once the size of the nuclei reaches a critical value, Au_{25} NCs start to form resulting in the rapid growth stage. The growth rate becomes slow and finally stops when no more Au_8 NCs can be consumed to form new nuclei. The rate constant is connected to temperature through the Arrhenius equation.

Table 1. Rate constants of gold NCs' transformation and Avrami components at different temperature.

Temperature (°C)	15	25	35
Rate constant $\times 10^6$ (s^{-1})	6.3 ± 0.6	19.2 ± 0.5	47.0 ± 1.0
Avrami component	1.60 ± 0.07	1.64 ± 0.06	1.53 ± 0.03

$$k = Ae^{-Ea/RT} \tag{3}$$

where A is the frequency factor, R the gas constant, and Ea the activation energy. The estimated Ea by plotting $\ln k$ against $1/T$ (see supporting information, figure S2) is around 74 kJ mol^{-1}. Recently, Zeng *et al* reported that the activation energies of the structural distortion and disproportionation are around 76 kJ mol^{-1} and 94 kJ mol^{-1} when

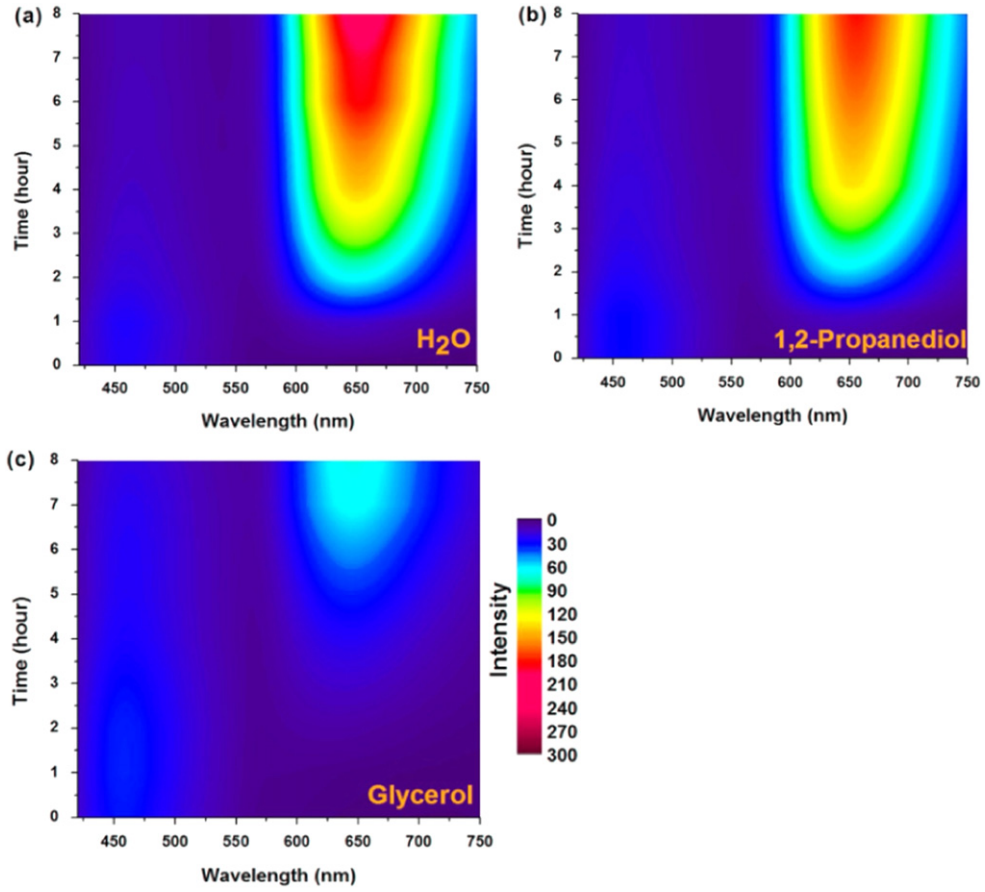

Figure 3. 2D fluorescence spectra contour plots in wavelength and time of the gold NCs' transformation process for 8 h at 35 °C excited at 390 nm with additional (a) H_2O, (b) 1, 2-propanediol and (c) glycerol.

$Au_{38}(SCH_2CH_2Ph)_{24}$ transforms into $Au_{36}(SPh\text{-}t\text{-}Bu)_{24}$ [28]. The greater stability of Au_{25} NCs compared to Au_8 NCs in an alkali environment is illustrated both in the structural and electronic aspects. When adding NaOH to Au_8 NCs' solution, positive charges in BSA are induced by the large amount of OH^- to establish a local electric field. The non-covalent interactions between Au_8 NCs and BSA are not stable enough to accommodate the strong electric field. The number of Au_8 NCs begins to decrease, and the disulfide bonds in BSA are broken in order to covalently bond with the gold [14, 17, 29]. After an initial nucleation stage, Au_{25} NCs are generated in the solution stabilized by a combination of Au-S covalent bonding with the cysteine residues in BSA.

3.3. Effects of solvent diffusivity

At each temperature, the Avrami component *n* estimated from the fitting curve of Au_{25} NCs' formation is very close to 1.5 (table 1), suggesting a diffusion-limited growth process [30, 31]. To confirm this result, three solvents with different viscosities are added immediately after mixing Au8 NCs with NaOH. The resulting pH is still 12. These mixtures are also kept at 35 °C for 8 h. The viscosity at 35 °C is 0.72 mPa s for H_2O, 20.27 mPa s for 1, 2-propanediol, and 405.78 mPa s for glycerol [32–34]. These solvents have no additional effects on Au_8 NCs or Au_{25} NCs (see details in supporting information, figure S3). The diffusivity is inversely proportional to the viscosity according to Stokes–Einstein equation [35]. Therefore, it is expected that higher viscosity will lead to lower diffusivity. Figure 3 shows the spectral reaction dynamics, demonstrating that low diffusivity (high viscosity) slows down the transformation process. When compared with H_2O, the consumption of Au_8 NCs and the formation of Au_{25} NCs presents a slight lag for 1, 2-propanediol (see details in supporting information, figure S4), and a significantly delay for glycerol. Chaudhari *et al* reported that after adding NaOH, the small gold NCs transform to larger ones with the emergence of free proteins indicating the interprotein gold transfer [13]. Some gold transfer from the original proteins leads to the occurrence of empty protein, and the aggregation around nucleation sites in other proteins to generate larger gold NCs. Xu *et al* demonstrated that only one gold NC exists in each BSA molecule [18]. Along with these facts, the data above suggest a possible transformation mechanism as: BSA protected Au_8 NCs existed in the aqueous solution when the pH was below 11. There were eight Au(0) atoms in each BSA molecule with only weak non-covalent bonding between them. In the presence of NaOH, the pH induced conformational change occurred inside BSA molecules. When the pH was increased to 11, nucleation sites started to appear in the activated Au_8 NCs attracting gold from other BSA molecules, possibly due to the purophilicity [36–38]. Once

the nucleation stage was complete, the growth process of Au_{25} NCs was initiated. Ostwald ripening (OR) and coalescence are two common growth models for metal nanoparticles (NPs) [39–44]. The researcher analyzed the UV-vis spectra accompanied by TEM images during the metal (Au or Ag) NPs' formation, and observed that a growth process based on the OR mechanism leads to a blue shift of the seed NPs' peak and is followed by continuous spectral shift [42, 44]. The blue shift indicated that the seed NPs dissolved into smaller ones, and continuous spectral shift was due to the size increasing. When Au_8 NCs transformed to Au_{25} NCs, neither blue shift or continuous spectral shift was observed in the fluorescence spectra. Spontaneous evolution of the band from Au_{25} NCs and simultaneous disappearance of the band from Au_8 NCs suggested a coalescence process [44]. Therefore, Au_8 NCs were directly used rather than decomposed first for the growth of Au_{25} NCs. However, there should be subsequent additional transformation modes leading to the final NC structure and further investigations are needed for future work. The inter-protein gold transfer mentioned above involved a long-range movement. The mobility of gold entering BSA was strongly affected by the diffusivity of the solution, resulting in a diffusion-controlled growth process. Meanwhile, this process was temperature dependent since a higher reaction temperature accelerated the molecule movement, resulting in a faster growth rate. At the end of the growth process, Au_{25} NCs covalently bonded with BSA molecules were generated with greater stability both structurally and electronically than Au_8 NCs.

4. Conclusion

In summary, we have studied the dynamic process of Au_8 NCs transforming into Au_{25} NCs, and their correlation with pH, reaction temperature and solvent diffusivity. When the pH changes from 8 to 12, the non-covalent bonding between Au_8 NCs and BSA is not strong enough that the number of Au_8 NCs begins to decrease. Meanwhile, Au_{25} NCs are generated with Au-S covalent bonding. By recording time-dependent fluorescence emission spectra at various temperatures and different solvent diffusivity, we demonstrate that Au_8 NCs are converted to Au_{25} NCs through an endothermic reaction with the activation energy of 74 kJ mol^{-1} using a diffusion-controlled growth mechanism, which can be illustrated by Avrami's theoretical model.

Acknowledgments

This work is financially supported by the Academia Sinica (AS) Nano Program and National Science Council (NSC) of Taiwan under the program No.102-2113-M-001-015 and No.99-2113-M-001-023-MY3. We would like to thank Ms C-Y Chien of the Precious Instrument Centre (National Taiwan University) for assistance with the TEM experiments.

References

[1] Parker J F, Fields-Zinna C A and Murray R W 2010 *Acc. Chem. Res.* **43** 1289
[2] Retnakumari A, Setua S, Menon D, Ravindran P, Muhammed H, Pradeep T, Nair S and Koyakutty M 2010 *Nanotechnology* **21** 055103
[3] Rongchao J 2010 *Nanoscale* **2** 343
[4] Yu J, Patel S A and Dickson R M 2007 *Angewandte Chemie-International Edition* **46** 2028
[5] Zheng J, Nicovich P R and Dickson R M 2007 *Ann. Rev. Phys. Chem.* **58** 409
[6] Wu Z and Jin R 2010 *Nano Lett.* **10** 2568
[7] Aikens C M 2008 *J. Phys. Chem.* C **112** 19797
[8] Lopez-Acevedo O, Tsunoyama H, Tsukuda T, Häkkinen H and Aikens C M 2010 *J. Am. Chem. Soc.* **132** 8210
[9] Zhu M, Aikens C M, Hollander F J, Schatz G C and Jin R 2008 *J. Am. Chem. Soc.* **130** 5883
[10] Baksi A, Xavier P L, Chaudhari K, Goswami N, Pal S K and Pradeep T 2013 *Nanoscale* **5** 2009
[11] Tkachenko A G, Xie H, Coleman D, Glomm W, Ryan J, Anderson M F, Franzen S and Feldheim D L 2003 *J. Am. Chem. Soc.* **125** 4700
[12] Brewer S H, Glomm W R, Johnson M C, Knag M K and Franzen S 2005 *Langmuir* **21** 9303
[13] Chaudhari K, Xavier P L and Pradeep T 2011 *ACS Nano* **5** 8816
[14] Xie J, Zheng Y and Ying J Y 2009 *J. Am. Chem. Soc.* **131** 888
[15] Bao Y, Zhong C, Vu D M, Temirov J P, Dyer R B and Martinez J S 2007 *J. Phys. Chem.* C **111** 12194
[16] Chen T-H and Tseng W-L 2012 *Small* **8** 1912
[17] Le Guével X, Hötzer B, Jung G, Hollemeyer K, Trouillet V and Schneider M 2011 *J. Phys. Chem.* C **115** 10955
[18] Xu Y, Palchoudhury S, Qin Y, Macher T and Bao Y 2012 *Langmuir* **28** 8767
[19] Yu Y, Luo Z, Teo C S, Tan Y N and Xie J 2013 *Chem. Commun.* **49** 9740
[20] Das T, Ghosh P, Shanavas M S, Maity A, Mondal S and Purkayastha P 2012 *Nanoscale* **4** 6018
[21] Mali B, Dragan A I, Karolin J and Geddes C D 2013 *J. Phys. Chem.* C **117** 16650
[22] Volden S, Lystvet S M, Halskau O and Glomm W R 2012 *RSC Advances* **2** 11704
[23] Wen X, Yu P, Toh Y-R, Hsu A-C, Lee Y-C and Tang J 2012 *J. Phys. Chem.* C **116** 19032
[24] Wen X, Yu P, Toh Y-R and Tang J 2013 *J. Phys. Chem.* C **117** 3621
[25] Tanaka A, Takeda Y, Imamura M and Sato S 2003 *Phys. Rev.* B **68** 195415
[26] Katchalski E, Benjamin G S and Gross V 1957 *J. Am. Chem. Soc.* **79** 4096
[27] Barbosa L R S, Ortore M G, Spinozzi F, Mariani P, Bernstorff S and Itri R 2010 *Biophys. J.* **98** 147
[28] Zeng C, Liu C, Pei Y and Jin R 2013 *ACS Nano* **7** 6138
[29] Simms G A, Padmos J D and Zhang P 2009 *J. Chem. Phys.* **131** 214703
[30] Christian J W 1995 *The Theory of Transformations in Metals and Alloys* (New York: Pergamon Press)
[31] Pelá R R, Cividanes L S, Brunelli D D, Zanetti S M and Thim G P 2008 *Materials Research* **11** 289
[32] Cheng N-S 2008 *Ind. Eng. Chem. Res.* **47** 3285
[33] Kestin J, Sokolov M and Wakeham W A 1978 *J. Phys. Chem. Ref. Data* **7** 941
[34] Khattab I S, Bandarkar F, Khoubnasabjafari M and Jouyban A 2012 *Arabian Journal of Chemistry* In press
[35] Su J T, Duncan P B, Momaya A, Jutila A and Needham D 2010 *J. Chem. Phys.* **132** 044506
[36] Schmidbaur H, Cronje S, Djordjevic B and Schuster O 2005 *Chem. Phys.* **311** 151

[37] Schmidbaur H 2000 *Gold Bulletin* **33** 3
[38] Runeberg N, Schütz M and Werner H-J 1999 *The Journal of Chemical Physics* **110** 7210
[39] Behafarid F and Roldan Cuenya B 2012 *Surf. Sci.* **606** 908
[40] Lotty O, Hobbs R, O'Regan C, Hlina J, Marschner C, O'Dwyer C, Petkov N and Holmes J D 2012 *Chem. Mater.* **25** 215
[41] Skrdla P J 2012 *Langmuir* **28** 4842
[42] Wang Y-C and Gunasekaran S 2012 *J. Nanoparticle Research* **14** 1200
[43] Zou G, Li H, Zhang D, Xiong K, Dong C and Qian Y 2006 *J. Phys. Chem.* B **110** 1632
[44] Lee G P, Shi Y, Lavoie E, Daeneke T, Reineck P, Cappel U B, Huang D M and Bach U 2013 *ACS Nano* **7** 5911